Cluster-glass state in manganites induced by *A*-site cation-size disorder

K. F. Wang, Y. Wang, L. F. Wang, and S. Dong
Laboratory of Solid State Microstructures, Nanjing University, Nanjing 210093, China

D. Li and Z. D. Zhang
Shenyang National Laboratory for Material Science, Institute of Metal Research and International Center for Materials Physics, Chinese Academy of Sciences, Shenyang 110016, China

H. Yu, Q. C. Li, and J.-M. Liu*
Laboratory of Solid State Microstructures, Nanjing University, Nanjing 210093, China and International Center for Materials Physics, Chinese Academy of Sciences, Shenyang 110016, China

(Received 12 September 2005; revised manuscript received 15 December 2005; published 11 April 2006)

The dependence of magnetotransport behaviors on *A*-site disorder induced by *A*-site cational size mismatch in ferromagnetic manganites is investigated by characterizing a series of samples with the same *A*-site cational mean radius $\langle r_A\rangle = 1.20$ Å but different *A*-site ionic radii variance $\sigma^2 = \Sigma_i x_i r_i^2 - \langle r_A\rangle^2$, where x_i and r_i are the atomic fraction and ionic radii of *i*-type ions at *A*-site, respectively. It is revealed that the ground state transits from ferromagnetic metal to cluster-glass insulator upon increasing the variance σ^2 from 0.0003 for $La_{0.55}Ca_{0.45}MnO_3$ to 0.015 for $Sm_{0.55}(Ca_{0.6}Ba_{0.4})_{0.45}MnO_3$, while the crystallographic structure and lattice constants of these manganites remain unchanged. Nevertheless, the increasing *A*-site disorder is believed to enhance the random local radial distortion of MnO_6 octahedra and suppress the ferromagnetic long-range order. In the manganites of high *A*-site disorder, the long-range ferromagnetic ordering is completely melted into the short-range magnetically ordered clusters and then the stepwise magnetization. With decreasing temperature, the short-range ordered clusters become frustrated at the frustrating point, below which a cluster-glass transition occurs due to the weak intercluster interaction.

DOI: 10.1103/PhysRevB.73.134411 PACS number(s): 75.30.Kz, 71.30.+h, 75.40.Cx

I. INTRODUCTION

Perovskite manganites, whose resistivity can change on the order of 10^4-10^6 by applying external magnetic field H of a few tesla, continue attracting the attention of condensed matter physicists.[1–3] This colossal magnetoresistance (CMR) effect can be qualitatively understood in the framework of the double-exchange interaction model (DE).[4] When the rare earth site (*A*-site) is doped with a divalent ion, a proportional number of Mn^{3+} ions are converted into Mn^{4+} ions and mobile e_g electrons are introduced, mediating the ferromagnetic (FM) interaction between Mn^{3+} and Mn^{4+} according to the DE interaction. In these manganite systems, the hopping of e_g electrons between two partially filled *d* orbitals of neighboring Mn^{3+} and Mn^{4+} ions via the orbital overlap e_g-O2p_σ-e_g, and the strong Hund coupling between the t_{2g} core spins and the mobile e_g electrons' spins cause the FM interaction between Mn^{3+} and Mn^{4+}.

However, recently it has been recognized that the phase diagram of manganites and many other strong correlated electron systems is multicritical, involving competing spin, charge, or orbital, and lattice orders.[5] The competition between these interactions and/or orders inherent in manganites, such as between double-exchange ferromagnetism and superexchange antiferromagnetism (AFM) and between charge-orbital ordered (CO-OO) state and metallic state, will produce the multicritical state.[6] In relation to the competition between the CO-OO state and FM metallic state (FMM), a scenario of the electronic phase separation has arisen as a generic feature of manganites. It has been accepted that, given a temperature T and magnetic field H, the electronic and magnetic ground state of manganites can be inhomogeneous due to the coexistence of FMM phase and CO-AF insulating (AFI) phase. The coexisting two phases originate from the electronic phase separation.[2,7,8]

On the other hand, the importance of the intrinsic disorder in the strong correlated mix-valence systems was recognized. The research on $Ln_{0.5}Ba_{0.5}MnO_3$, where Ln and Ba ions can form either an ordered or a disordered structure, reveals the significant disordered effects in manganties.[9] In the ordered phase or "clean limit," where Ln and Ba ions form a periodic layered structure, the phase diagram shows a multicritical behavior where FMM and CO-OO state compete with each other. For the disordered case, where the arrangement of (Ln, Ba) ions is completely random, the diagram changes in a very asymmetric manner: FMM phase is partially suppressed but still survives at finite temperature, while the CO-OO state disappears and instead some glassylike state is realized at low temperature. The enhanced CMR effect is observed in the region where the disorder induces the transition from CO-OO to FMM. Earlier research revealed that the site disorder not only produces the glassy state but also enhances the fluctuation of the competition orders, i.e., between the CO-OO and FMM states, near the original bicritical point.[10–15] Such a large fluctuation is amenable to an external field favoring the FMM phase and may be one of the most essential ingredients of the CMR physics. In fact, the disorder introduced by Mn-site doping was studied carefully. The Cr doping on Mn site gives rise to the FM clusters coexisting with the CO-OO background.[14,15] The doping with the non-

TABLE I. Summary of chemical, structural and physical data for the $RE_{0.55}AE_{0.45}MnO_3$ series with a constant A-site cation mean radius $\langle r_A\rangle = 1.20$ Å.

Composition	σ^2 (Å^2)	T_{MI} (K)	T_C (K)	T_f (K)	$M(T=3\text{ K})$ (μ_B per formula unit)
$La_{0.55}Ca_{0.45}MnO_3$	0.0003	228.7	232.6		3.48
$Nd_{0.55}(Ca_{0.45}Sr_{0.55})_{0.45}MnO_3$	0.003	200.8	194.5		3.36
$Sm_{0.55}(Ca_{0.2}Sr_{0.8})_{0.45}MnO_3$	0.007	105.7	115.5		2.82
$Nd_{0.55}(Ca_{0.76}Ba_{0.24})_{0.45}MnO_3$	0.008			42.0	2.62
$Gd_{0.55}Sr_{0.45}MnO_3$	0.009			42.0	1.51
$Sm_{0.55}(Ca_{0.6}Ba_{0.4})_{0.45}MnO_3$	0.015			42.5	1.01

magnetic Ga ions makes the first-order transition in $La_{2/3}Ca_{1/3}MnO_3$ continuous,[11] and the long-range FM phase coexists with short-range magnetic correlations in the low doping level.[12] So, the first-order transition in pure $La_{2/3}Ca_{1/3}MnO_3$ is induced by fluctuations from competition.[11] Theoretical approaches also predicted that the disorder in the critical region may produce phase coexistence of two competing ordered phases on various time and length scales.[16–18]

In addition to the B-site doping and Ba-based manganites, the A-site cation size disorder can also be interesting. Hereafter, the A-site cation size disorder (in short, the A-site disorder) is designated to the disorder induced by A-site ionic radii mismatch. It has been proven that the variance of the A-site ionic radii, $\sigma^2 = \Sigma_i x_i r_i^2 - \langle r_A\rangle^2$, where x_i and r_i are the atomic fraction and ionic radii of i-type ions at A-site, respectively, govern the magnetic and transport properties of manganites, and thus can be defined as the parameter to characterize the A-site disorder. In fact, earlier works often took the tolerance factor $t = (\langle r_A\rangle + r_O)/\sqrt{2}(r_{Mn} + r_O)$ as a parameter to interpret the relationship between the magnetotransport behaviors and lattice structure of manganites. Although this tolerance factor is related to the A-site cation mean radius $\langle r_A\rangle$, no A-site disorder is taken into account.[19–21] It was also reported that the temperature T_m of the transition from FMM to paramagnetic (PM) insulator varies as $T_m = T_m(0) - pQ^2$ due to the strain fields resulting from ordered or disordered oxygen displacements Q that are parametrized by the statistical mean and variance of the A-cation radius, respectively.[19] In this case, the effect of the A-site disorder on the transition temperature T_m is explained.

Compared with the Mn-site doping, the A-site cational size mismatch can introduce the disorder over a wide range and then the local lattice distortion can be modulated to a large extent. But, this mismatch does not cause significant change of the crystallographic structure and lattice constants, in the sense of x-ray diffraction (XRD) over a macroscopic volume of sample. Neither magnetic impurity nor change of the Mn^{3+}/Mn^{4+} ratio will be possible. Therefore, a study on the A-site disorder may be a more direct and purified roadmap to understand the physical mechanism associated with disorder in manganites. One may expect that the A-site disorder can lead to the same effects as by the Mn-site disorder, such as cluster-glass behavior and phase-separated state.

As mentioned above, the effects of the A-site disorder in manganites were previously investigated.[19,20] However, previous studies only pointed out the relevance between T_m and the A-site disorder; not much data on phase separation behaviors associated with the A-site disorder are available so far. In particular, to the authors' best knowledge, no experimental evidence on the cluster-glass ground state at low temperature as induced by the A-site disorder has been reported. It is expected that the A-site disorder may not only suppress the ferromagnetic transition but also prefer the localization of electrons. In this paper, the effect of A-site disorder over a broad range in ferromagnetic manganites will be investigated by preparing a series of samples which have the same A-site cation mean radius $\langle r_A\rangle = 1.20$ Å but different values of variance σ^2 ranging from 0.0003 to 0.015 Å^2. One of the experimental findings is that a destabilization of the FM metal ground state is indeed possible by mediating the A-site disorder.[22] We shall present in this work detailed experimental evidence on the transitions of the ground state from FM metal to low-temperature spin cluster-glass insulator in manganites with high A-site disorder.

This paper is organized as follow. We report the sample preparation and property characterizations using various techniques in Sec. II. The multifacet experimental evidence and discussions on the low-temperature cluster-glass state induced by the A-site disorder will be presented in Sec. III, followed by a conclusion in Sec. IV.

II. EXPERIMENTAL PROCEDURES

A series of samples which have a constant A-site cation mean radius $\langle r_A\rangle = 1.20$ Å but different values of variance σ^2 as shown in Table I was chosen for the present study. The values of radius and variance σ^2 were calculated using standard nine-coordinated cation radii.[23] All the ceramic samples were prepared by the conventional solid-state reaction in air. The highly purified powders of oxides-carbonates were mixed in stoichiometric ratios, ground, and then fired at 1250 °C for 24 h in air. The resultant powders were reground and pelletized under 3000 psi pressure to disks of 1 cm in diameter; then, the pellets were sintered at 1400 °C in air for 12 h.

In order to check whether our samples have the same A-site cational mean radii and then the same lattice parameters, high-resolution XRD with Cu $K\alpha$ radiation at room temperature on these samples was performed, assisted by careful lattice structure characterization using the Rietveld refining method.

The effects of the *A*-site disorder on the transport and magnetization of all the samples were studied carefully. The transport measurements were performed using a standard four-probe method down to 20 K under zero field and a magnetic field $H=6$ T using a MPMS (magnetic properties measurement system). The magnetic property including the ac susceptibility as a function of temperature T and H was also measured using a Quantum Design SQUID (superconducting quantum interfering device). In the zero-field cooled (ZFC) measurements the samples were cooled from ~300 to 3 K under zero field, and then the ZFC magnetization measurements were performed in the warming process with a field of $H=100$ Oe. For the field-cooled (FC) cases, the samples were first cooled to 3 K in the presence of $H=100$ Oe; then, the magnetization was probed under the same field during the heating cycle. The magnetic loops were recorded at 3 K from $H=0$ to 7 T after the ZFC sequence.

III. RESULTS AND DISCUSSION

A. Crystal structure

In Fig. 1(a) we present the XRD θ-2θ patterns measured at room temperature for a set of samples with different values of variance σ^2 (*A*: 0.003, *B*: 0.007, *C*: 0.008, *D*: 0.009, *E*: 0.015). The unit of σ^2 is Å^2 hereafter unless stated otherwise. All the samples are well crystallized with pure orthorhombic structure with space group *Pbnm*. No identifiable reflection shift upon increasing variance σ^2 is observed, which demonstrates no change of the crystallographic structure and lattice constants on variance σ^2. To confirm this effect, we perform the Rietveld refinement[23] on the diffraction spectra. The data on two samples ($\sigma^2=0.007$ and 0.009) are shown in Figs. 1(b) and 1(c), where the open circle dots represent the measured XRD reflections and the solid lines are the Rietveld refined results. Very small difference is shown between the measured spectra and refined ones. The reliability of the Rietveld refinement is demonstrated by the high-quality refinement parameters $R_p=11.3\%$, $R_{wp}=12.4\%$, and $S=1.19$ for the sample of $\sigma^2=0.007$, and $R_p=10.8\%$, $R_{wp}=16.4\%$, and $S=1.19$ for the sample of $\sigma^2=0.009$. The lattice parameters at room temperature as obtained by the refinement are $a=5.4831(5)$ Å, $b=5.4706(3)$ Å, $c=7.7283(6)$ Å for the sample of $\sigma^2=0.007$. For the sample of $\sigma^2=0.009$, they are $a=5.4763(7)$ Å, $b=5.4682(6)$ A, $c=7.7266(3)$ Å. It is revealed that the volume change associated with the variation of σ^2 from 0.0003 to 0.015 is less than 0.5%.

The argument that the crystallographic structure is independent of variance of σ^2 is based on the XRD data averaged over a macroscopic volume of the samples. It does not mean that no local lattice distortion occurs due to different σ^2. However, the distortion of local lattices is spatially random over the whole sample, resulting in the invariance of the XRD-probed lattice structure in the macroscopically averaged sense. We shall return to this issue below, and will see that the influence of the *A*-site disorder on the local structure distortion can be significant, as characterized by the tremendous change of the transport and magnetic properties.

It is therefore concluded that, given the constant *A*-site cation mean radius $\langle r_A\rangle=1.20$ Å, the variation of the *A*-site disorder as characterized by variance σ^2 causes no change of the crystal structure. The lattice parameters remain nearly unchanged as well.

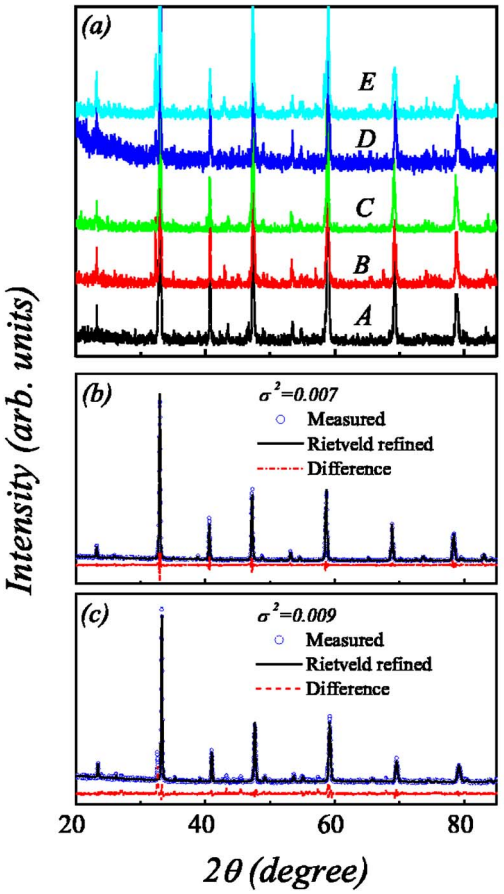

FIG. 1. (Color online) (a) X-ray diffraction θ-2θ spectra at room temperature for a series of samples of variance σ^2 (from bottom to top): (A) 0.003; (B) 0.007; (C) 0.008; (D) 0.009; and (E) 0.015. (b) Measured XRD θ-2θ spectrum (open circle dot, measured) and evaluated spectrum (solid line, Rietveld refined) using Rietveld structural refinement for sample of $\sigma^2=0.007$. (c) Measured and Rietveld refined spectra for sample of $\sigma^2=0.009$. The difference (dashed line, difference) between the measured and Rietvield refined spectra for the two samples, respectively, is plotted with a slightly downshift for clarity in (b) and (c). The unit of σ^2 is Å^2.

B. Metal-insulator transition

We measured the zero-field resistivity ρ as a function of T for all samples over the T range from 20 to 300 K; the results are shown in Fig. 2(a). An overall comparison of the data demonstrates the significant effect of the *A*-site disorder on the transport behaviors. In general, one sees an overall increasing of ρ with increasing σ^2. For the sample $La_{0.55}Ca_{0.45}MnO_3$ ($\sigma^2=0.0003$), the T dependence of ρ exhibits the typical insulating behavior in the high-T range. The resistivity ρ reaches the maximum at $T=T_{MI}=228.7$ K and decreases with further decreasing of T, where T_{MI} is the metal-insulator transition (MIT) point, noting that the measured T_{MI} is in agreement with earlier reported data.[2] Similarly, the samples $Nd_{0.55}(Ca_{0.45}Sr_{0.55})_{0.45}MnO_3$ ($\sigma^2=0.003$)

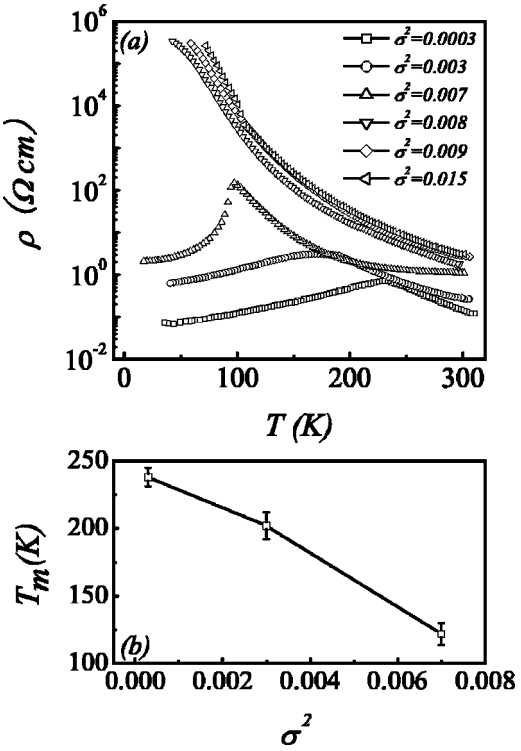

FIG. 2. (a) Zero-field resistivity ρ as a function of T for all the samples with σ^2 from 0.0003 to 0.015. (b) Measured dependence of T_m on σ^2. The unit of σ^2 is Å^2.

and $Sm_{0.55}(Ca_{0.2}Sr_{0.8})_{0.45}MnO_3$ (σ^2=0.007) again show the MIT behavior, with T_{MI} decreasing from 201 to 106 K, as shown in Fig. 2(b), where the uncertainties for T_{MI} are also inserted. Referring to sample $Nd_{0.55}(Ca_{0.76}Ba_{0.24})_{0.45}MnO_3$ for which σ^2=0.008, no MIT behavior can be observed and the insulator ground state is kept over the whole T range. Further increasing σ^2 only causes the increase of ρ. The samples $Gd_{0.55}Sr_{0.45}MnO_3$ (σ^2=0.009) and $Sm_{0.55}(Ca_{0.6}Ba_{0.4})_{0.45}MnO_3$ (σ^2=0.015) remain insulating over the whole T range too.

The significantly different transport behavior upon different values of σ^2 as shown above allows us to argue the essential role of the A-site disorder in mediating the phase separation of ferromagnetic manganites, noting that no charge-ordered phase appears upon increasing the A-site disorder. Therefore, we turn to the magnetic behaviors of these samples in order to reveal the magnetic ground state in the manganites of different A-site disorder degrees.

C. Magnetization behavior

Figure 3 shows the T dependence of the dc magnetization M for samples of σ^2=0.0003, 0.007, 0.008, 0.015. The samples with small A-site disorder degree (σ^2=0.0003 and 0.007) exhibit a PM-FM transition at T_m=232.6 and 122.9 K, respectively (T_m was determined using the Lorentzian function fit of the derivation curves). Increasing σ^2 causes a decrease of T_m, which is in accordance with the MIT transition point shown in Fig. 2(b). As σ^2 further increases, the M-T curves at ZFC cases show a cusplike peak

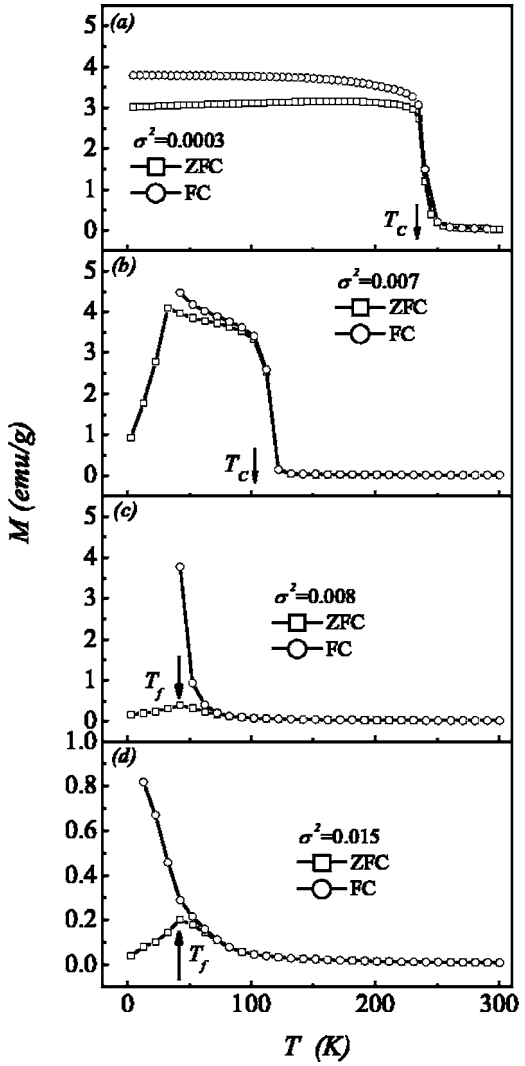

FIG. 3. Measured magnetization M as a function of T measured during warm cycle for samples of (a) σ^2=0.0003; (b) 0.007; (c) 0.008; (d) 0.015; respectively, under the ZFC and FC conditions. The unit of σ^2 is Å^2.

at about $T=T_f\sim$42 K when σ^2 is higher than 0.008. This effect immediately allows us to argue a possible spin-glass-like transition occurring at T_f. In fact, similar peaks were observed at the cluster-glass transition for $La_{2/3}Ca_{1/3}MnO_3$ with Ga, Al, and Fe doping at the Mn site, respectively.[12,24,25] Notice that for all the samples there appears an irreversibility between the ZFC and FC magnetization curves. However, this irreversibility is very small at small σ^2, even at temperature below the cusplike peak. It becomes remarkable for the samples of σ^2=0.008 and 0.015 once T is down close to T_f. Such an irreversibility of the magnetization is one of the typical features of the spin-glass-like state.[26,27]

The H dependences of magnetization M at T=3 K for the samples of σ^2=0.003, 0.007, 0.008, and 0.015, measured through the field-increasing and field-decreasing cycle, are shown in Fig. 4. For σ^2=0.003 and 0.007, the saturated M is achieved at H=1 T and higher. However, at σ^2=0.008, M remains unsaturated until H=3.5 T, at which a stepwise behavior occurs. Afterwards, the magnetization becomes satu-

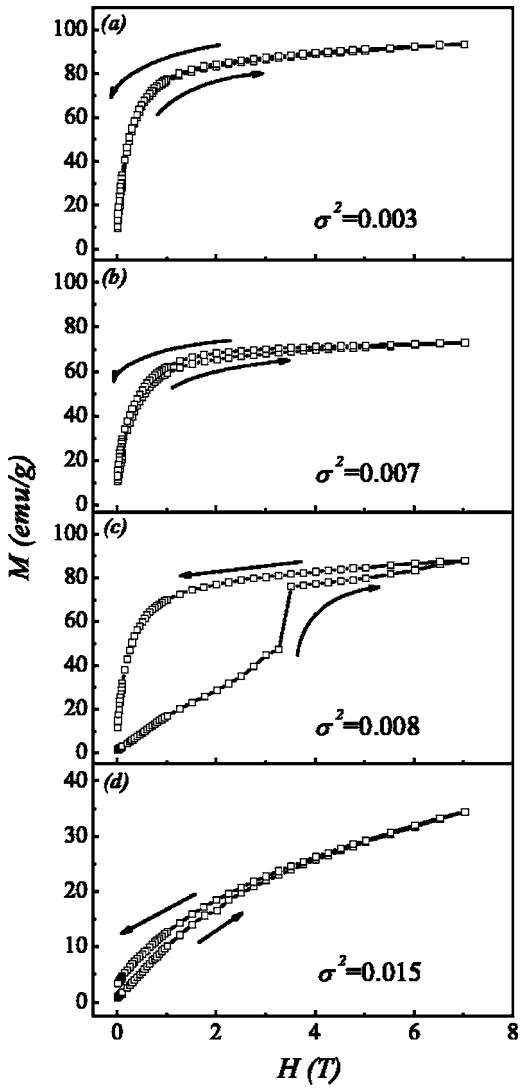

FIG. 4. Measured magnetization M as a function of H at $T=3$ K for samples of (a) $\sigma^2=0.003$; (b) 0.007; (c) 0.008; and (d) 0.015, respectively. The arrows indicate the cycle of H varying during measurements. The unit of σ^2 is Å^2.

rated. Nevertheless, for the samples of $\sigma^2=0.009$ and 0.015, no saturated magnetization can be reached even at a field as high as $H=6.0$ T.

It is known that the high-spin Mn gives spin-ordered moment $\mu=gs\mu_B$ (orbital contribution quenched) where Mn^{3+} and Mn^{4+} carry $4\mu_B$ and $3\mu_B$, respectively. If all Mn ions were in a FM state, the maximum spin-only ordered moment would be $3.55\mu_B$ per formula unit and the magnetic moment should remain constant ($=3.55\mu_B$), because all the samples have the same Mn^{4+}/Mn^{3+} ratio. However, the measured M at $T=3$ K and $H=3$ T is found to be 3.48, 3.36, 2.82, 2.62, 1.51, and $1.01\mu_B$ per formula unit for $\sigma^2=0.0003$, 0.003, 0.007, 0.008, 0.009, and 0.015, respectively, as shown in Table I and Fig. 5. An abrupt decrease of M as a function of σ^2 occurs at $\sigma^2\sim0.008$. As $\sigma^2=0.015$, the measured M becomes very small. Simultaneously, the zero-field resistivity shows an abrupt increases at $\sigma^2\sim0.008$, as shown in Fig. 5.

Keeping in mind the above data on the transport and magnetization, we can argue that the low-T ground state for the

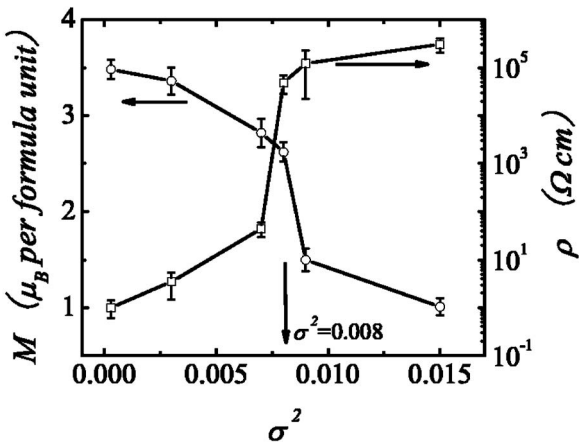

FIG. 5. σ^2 dependences of magnetization M measured at $T=3$ K under a field $H=3$ T, and zero-field resistivity ρ measured at $T=50$ K. The unit of σ^2 is Å^2.

manganites of large σ^2 is neither AFM state nor FM state, excluding trace with any charge-ordered state. Instead, the spin-glass-like state becomes the ground state for these manganites. In order to provide further evidence for this argument, we measured the ac magnetic susceptibility χ_{ac} as a function of T at different frequencies (10, 100, 500, and 1000 Hz) for all the samples. The measured results do reveal the typical features of spin-glass-like behavior at low T for those sample of $\sigma^2\geqslant0.008$. In Figs. 6(a) and 6(b) the data are plotted for the samples of $\sigma^2=0.008$ and 0.009, respectively. The peaked pattern and significant frequency-dispersion feature of the χ_{ac}-T curves support our above argument on the spin-glass-like state as the ground state at low T.

The ac susceptibility data also allow us to give a rough estimate of the time scale for magnetic relaxation. From Fig. 6 we observe the peak shift toward the high temperature with increasing frequency. Given an assumption that the spin-glass follows the thermally activated relaxation, one has the relaxation time τ according to the Néel-Arrhenius law,

$$\tau=\tau_0\exp(E/k_BT_P), \tag{1}$$

where ω is the driving frequency for measuring χ_{ac}, $\tau=1/\omega$, and T_P is the peak temperature. Prefactor τ_0 depends on the gyromagnetic precession time and is usually $\sim10^{-200}$ s for typical spin-glass, although this time scale is not sound physically if one employs the Néel-Arrhenius law to estimate the value of τ_0. If $\tau_0\sim10^{-10}$–10^{-13} s, the system would be of superparamagnetism, which is composed of noninteracting magnetic particles or clusters with a temperature-dependent distribution of the relaxation times.[27] Our fitting results using this law, shown in Fig. 6(c), give an estimated value of $\tau_0\sim10^{-100}$ s, far shorter than the 10^{-10}–10^{-13} s for the superparamagnetic case, but much longer than that for the typical spin glass. This indicates that the low-T ground state of our highly A-site disordered samples is not typical spin-glass but is composed of magnetic clusters with weak intercluster interactions, i.e., the cluster-glass state. The magnetic transition for the samples

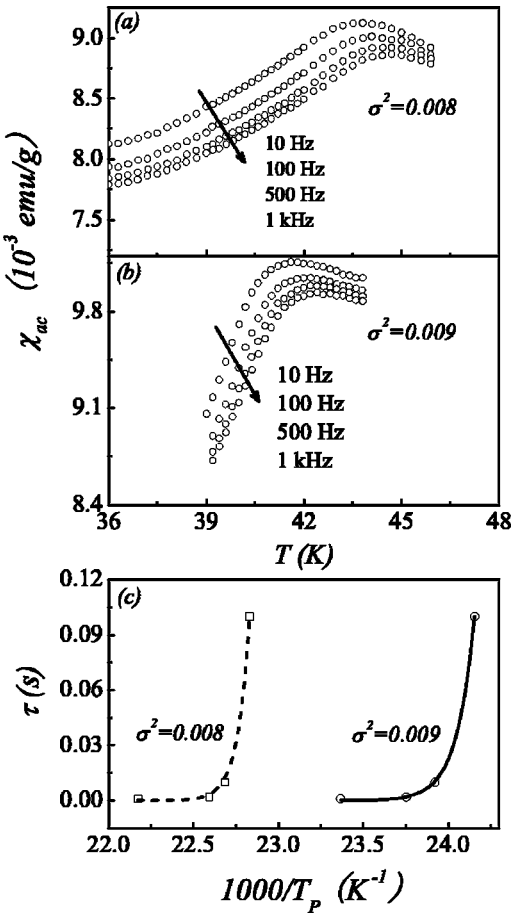

FIG. 6. Measured ac susceptibility χ_{ac} as a function of T at four frequencies (10, 100, 500, and 1000 Hz) for samples of (a) $\sigma^2=0.008$ and that of (b) $\sigma^2=0.009$, respectively. (c) Evaluated relaxation time τ as a function of T_P (open dot) and fitting curves (lines) using the Néel-Arrhenius law. The unit of σ^2 is Å^2.

with $\sigma^2=0.008$, 0.009, and 0.015 is essentially ascribed to the collective frustrating.[27]

Based on all the magnetic and transport measurements presented above, we may conclude that upon increasing A-site disorder, i.e., increasing σ^2 from 0.0003 to 0.015, the ground state evolves from a FMM state to a cluster-glass-like insulator. This experimental finding demonstrates the essential significance of the A-site disorder, similar to the B-site disorder, in modulating the ground state of manganites.

D. Disorder induced cluster-glass like transition

To understand the physics associated with the A-site disorder, we may look back to the classical picture of manganites. One of the key parameters to determine the ground state in manganites is the transfer interaction of the e_g state conduction electron between neighboring Mn sites or the effective one electron bandwidth (W) of the e_g band. The bandwidth W, which is dependent on the lattice distortion of the perovskite structure, can be described as

$$W = \cos\left(\frac{1}{2}\pi - \langle\beta\rangle\right) \Big/ d_{\text{Mn-O}}^{3.5}, \tag{2}$$

where $\langle\beta\rangle$ is the average angle of the Mn-O-Mn bond, $d_{\text{Mn-O}}$ is the average length of the Mn-O bond which can be modulated by $\langle r_A\rangle$. Since the DE interaction responsible for the FMM state is scaled by W,[28,29] the stability of the FM state in a distorted perovskite manganite will be damaged, and the ground state is often replaced by competing phases against FM, such as CO-OO antiferromagnetic insulator (AFI). A typical case is that a reduction of $\langle r_A\rangle$ from the ideal value will lead to ordered oxygen displacement and then a CO-OO AFI state.

However, this picture is contradictory to our experimental results. All the samples studied here have the same $\langle r_A\rangle = 1.20$ Å, which is very close to the ideal value, and thus the same W. The XRD-probed crystal structure of all the samples also remains the same. Unfortunately, our experiments revealed that the samples with different A-site disorders exhibit completely distinct properties. In fact, in MnO_6 octahedra, besides the reduction of $\langle r_A\rangle$, the size difference between two neighboring A-site R^{3+} and M^{2+} ions around one oxygen ion can result in oxygen displacement too, and then can result in local distortion of MnO_6 octahedra or bending of the Mn-O-Mn bond in these octahedra.[20] In our samples, the different A-site ions with different radii are randomly distributed; thus, the mode and magnitude of the MnO_6 octahedra distortions or the Mn-O-Mn bond bending are spatially random and inhomogeneous. The sample of small variance (e.g., $\sigma^2=0.0003$ and 0.003), in which the MnO_6 octahedra distortion is weak, certainly exhibits the typical properties of the large-bandwidth manganites, such as MIT accompanied by a FM-PM transition. As σ^2 becomes larger, the local MnO_6 octahedra distortion becomes more serious and the number of distorted MnO_6 octahedra increases, i.e., the A-site disorder increases. Therefore, the Mn ions around the distorted MnO_6 octahedra may no longer be able to participate in the DE process.

A direct consequence of the above effect is the decrease in T_m (or T_{MI}) with increasing variance σ^2, because the local strain contribution to the transition enthalpy is suppressed.[20] In such case the decrease in T_m is roughly linear, following $T_m = T_m(0) - pQ^2$.[20] The measured data presented above agree with this prediction, as shown in Fig. 2(b). Furthermore, because of the increasing disorder, the reduction in the number of lattice sites participating in the itinerant DE interaction and then the dilution of the DE network for electron conduction would suppress the system magnetization and conductivity, as revealed in our experiments too.

However, it is worth noting that a dilution of the DE network may not be the only sequence of the cation disorder. If the disorder would only produce a dilution, the FMM state should be able to survive up to much higher disorder level than what we observed above: $\sigma^2 \sim 0.007$. Taking into account that the FM state is often replaced by CO-OO AFI in distorted manganites, the Mn ions around the distorted MnO_6 octahedra may prefer locally short-range CO-OO AFI state. This means that the A-site disorder destablizes the long-

range FM order which maintains as $\sigma^2 \leqq 0.007$. Once $\sigma^2 > 0.008$, the short-range magnetically ordered phase becomes favored.

An additional evidence on the above argument is the stepwise behavior in the *M-H* loops for sample $Nd_{0.55}(Ca_{0.76}Ba_{0.24})_{0.45}MnO_3$, which has an intermediate disorder level $\sigma^2 = 0.008$. The magnetization as a function of H exhibits a sharp step at $H \sim 3.5$ T. Such a stepwise behavior was once observed in manganites like $Pr_{0.55}Ca_{0.45}MnO_3$,[30] $Pr_x(Ca, Ba/Sr)_{1-x}MnO_3$,[31] $Pr_xCa_{1-x}(Mn, Co/Cr/Ga)O_3$,[32–34] $(La, Pr/Bi)_{0.67}Ca_{0.33}MnO_3$,[35,36] etc. For these manganites, the martensitic scenario based on phase separation can be used to explain the observed effect.[34] The FM phase which has more symmetrical perovskite domains (i.e., with weaker orthorhombic distortion) can coexist with the strongly distorted CO-OO AFI regions.[2] Upon application of a magnetic field, the symmetrical perovskite domains become ferromagnetic, but the expansion of the FM phase is stopped by the interfacial strains on the boundaries between the FM and AFI regions, due to the possible strongly distorted regions on the boundaries. It is necessary for H to go beyond a critical value in order to get over the strain energy and enforce a further expansion of the FM regions. A sharp magnetization step is then observed, which is an indication of the coexistence of the long-range ordered FM regions and short-range CO-OO AFI regions in the sample with an intermediate disorder.

With further increasing of the *A*-site disorder, the long-range FM ground state is completely melted into the short-range magnetically ordered regions. The system can no longer develop sufficient symmetrical domains to induce the FM ordered regions. Consequently, M remains very low ($\sim 1.01 \mu_B$ for sample with $\sigma^2 = 0.015$ under $H = 4.0$ T). Very similar to typical cluster-glass systems, the short-range magnetically ordered regions in the present samples may frustrate when temperature falls to a frustrating point at which these regions begin to freeze due to the intercluster frustration. The cluster-glass transition is thus activated. Below this point, the sample exhibits a cluster-glass-like behavior in terms of the transport and magnetic properties. In short, the increasing *A*-site disorder makes the ground state transform from metal to insulator (MIT), which occurs around $\sigma^2 \sim 0.008$. The long-range FM state for $\sigma^2 < 0.007$ will melt into the short-range magnetically ordered clusters as $\sigma^2 > 0.009$. At $\sigma^2 \sim 0.008$, the coexistence of both states is observed. This behavior seems typical for an electron localization process.

E. Transport evidence on the cluster-glass-like transition

The high-temperature transport data of the samples can be used to check the above argument on the cluster-glass ground state in highly *A*-site disordered manganites. The *A*-site disorder brings about the electron localization that suppresses the DE interaction. The abrupt MIT of the ground state as a function of σ^2 is remarkable (as shown in Fig. 5) and mimics the typical MIT induced by the electron localization. Given the argument that the *A*-site disorder induces the transform of the long-range FM regions to short-range magnetically ordered regions, one may propose that the conduction follows the variable-range-hopping (VRH) model,[37]

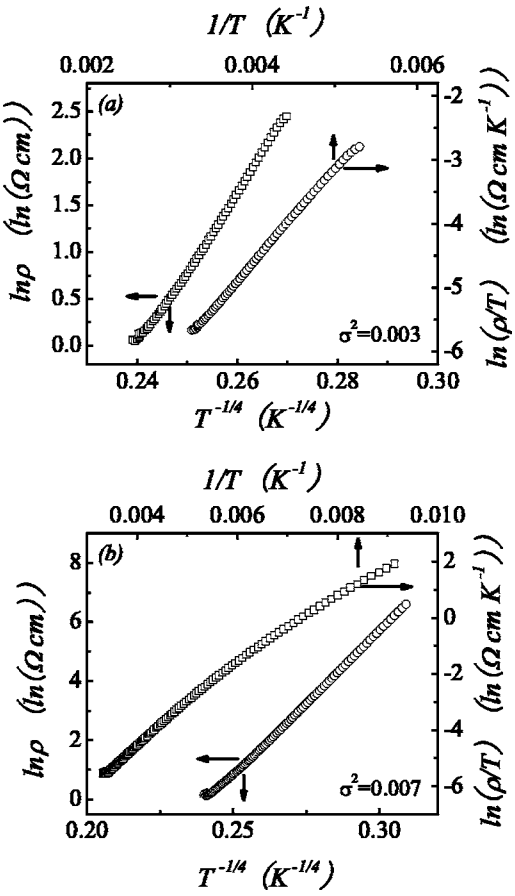

FIG. 7. Fitting of zero-field resistivity ρ as a function of T using the VRH model and small-polaron model for samples with (a) $\sigma^2 = 0.003$ and (b) 0.007. The unit of σ^2 is Å^2.

$$\rho = \rho_{i0} \exp[(T_0/T)^{1/4}], \tag{3}$$

where ρ_{i0} is the prefactor and T_0 is the characteristic temperature. Otherwise, the small-polaron model should be followed by the conduction,[38] which reads

$$\rho = \rho_0 T \exp(-E_0/kT), \tag{4}$$

where ρ_0 is the prefactor, E_0 is the activation energy of the small polaron, and k is the Boltzmann constant.

Plots of $\rho(T)$ data for the samples with $\sigma^2 = 0.003$ and 0.007 according to both the VRH and the small-polaron model are presented in Fig. 7. For $\sigma^2 = 0.003$, the data agree well with the prediction of both the VRH and the small-polaron mechanism; it is impossible here to make an identification of the conduction mechanism only from the transport behavior. However, the conduction for the $\sigma^2 = 0.007$ sample simply follows the VRH rather than the small-polaron model. Over the whole insulating T-range, a good $\ln \rho \sim T^{-1/4}$ relationship is identified, whereas no satisfactory $\ln(\rho/T) \sim T^{-1}$ behavior is observable. The $\rho(T)$ data for the samples with $\sigma^2 = 0.008$ and 0.009 according to the VRH are shown in Fig. 8. The good linear behavior apart from the data at very low-T range indicates that the *A*-site disorder is bringing about the electron localization and formation of the short-range magnetically ordered clusters.

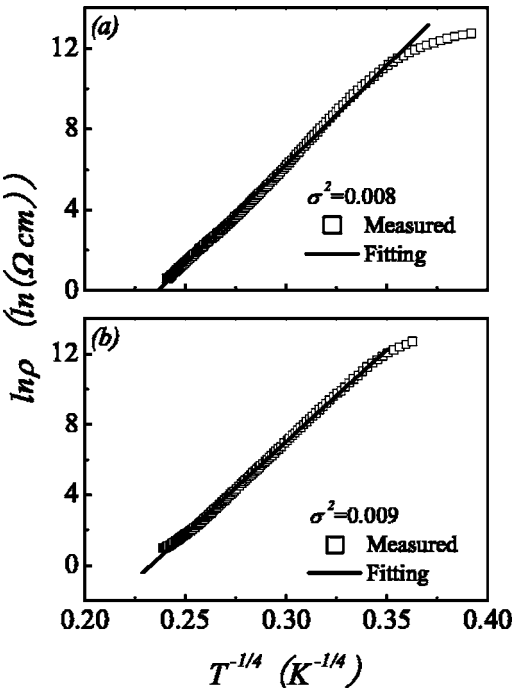

FIG. 8. Fitting of zero-field resistivity ρ as a function of T using the VRH model for samples with (a) σ^2=0.008 and (b) 0.009. The unit of σ^2 is Å^2.

F. Disorder enhanced CMR effect

In addition, it is worthy to note the CMR effect induced by the A-site disorder. Figure 9 shows the measured ρ-T curves at H=0 and H=6 T, and also the evaluated magnetoresistance (MR) ratio defined as $MR=[\rho(0)-\rho(H)/\rho(0)]$ as a function of T, for the samples with σ^2=0.003, 0.007, and 0.008, respectively. We can see the sample of σ^2=0.003 exhibit typical CMR effects: field H induces shifting of the MIT point to higher temperature and huge decrease of the resistivity. The MR-T curve exhibits a peak at the MIT point. The peaked MR ratio is ~70% at a field of H=6.0 T. For the sample of σ^2=0.007, the measured MR value is ~92% but reached at lower T.

As $\sigma^2 > 0.008$, the ground state prefers the cluster-glass-like state, as demonstrated above. Over the high-T range, the observed MR effect is not significant. However, it is noticed that the sample in low-T range shows a fantastic effect: a field of H=6 T enforces the ground state to change from an insulator to a metal, and a clean MIT effect is observed under H=6 T. The induced MR is very huge and reaches almost 100% (~99.9%) below the MIT point. This huge CMR effect is obviously the outcome of the competition between the FM and AFI regions. As σ^2 is even larger, no MIT effect can be observed at a field of 6 T, the highest field available to us in our experiments.

G. Remarks and discussion

It is well known that the sample with the lowest A-site disorder in our experiments, $La_{0.55}Ca_{0.45}MnO_3$, is adjacent to the boundary between the FM phase and CO-OO AFI phase in its phase diagram.[2] There may exist competition between

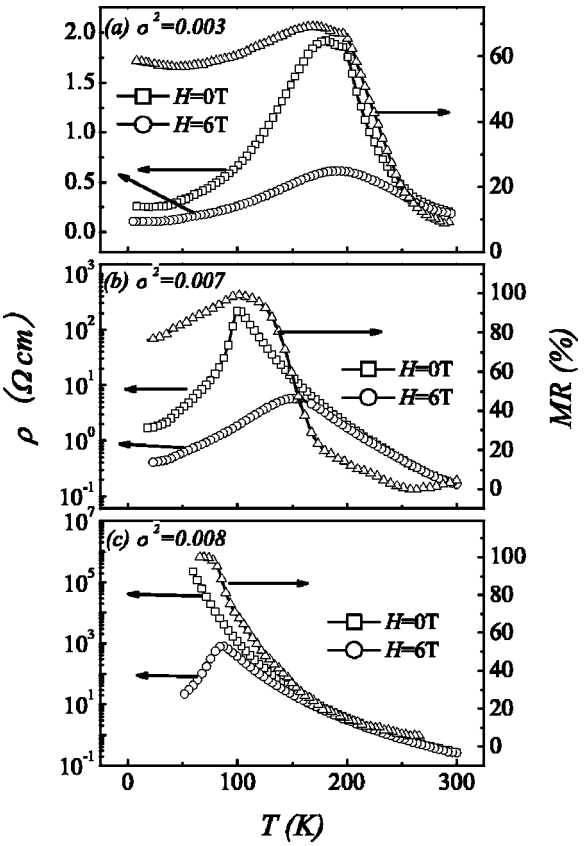

FIG. 9. Measured $\rho(H=0)$ and $\rho(H=6$ T) as a function of T for samples of (a) σ^2=0.003; (b) σ^2=0.007; and (c) σ^2=0.008, respectively. The MR ratio for each sample is plotted in the same figure. The unit of σ^2 is Å^2.

the FM double-exchange interaction and the AFM superexchange interaction, which favor the long-range FM order and A-type AFM order, respectively. Therefore, the A-site disorder results in a crossover from a long-range ordered state to a state with short-range ordered clusters. For the intermediate disorder case, there probably exists a Griffiths phase which can be characterized by an inhomogeneous magnetic state at the microscopic scale with coexisting clusters of the competing ground states.[39] This Griffiths phase will appear before the system is dominated by the cluster-glass state, with increasing variance σ^2.

The existence of a Griffiths phase can be most directly evidenced by means of small-angle neutron scattering (SANS) and nanoscale high-resolution magnetic force microscopy, which are unfortunately not available to us. Here, we present indirect evidence on the Griffiths phase by analyzing the susceptibility χ as a function of T under low magnetic field, which could characterize the Griffiths phase.[40] Figure 10 shows the measured $1/\chi$ as a function of T for the samples with σ^2=0.0003 and 0.007 measured under H =100 Oe, noting here that the ground state at σ^2=0.008 is already the cluster-glass state, as shown above. If these data follow the Curie-Weiss law, they would lie on a straight line given by $1/\chi=\frac{3k_BT_C}{g\mu_B(S_{eff}+1)}\left(\frac{T}{T_C}-1\right)$, where S_{eff} is the effective spin, g is the Lander factor, μ_B is the Bohr magnetron, and T_C is the Curie point. In Fig. 10 the dashed lines are the

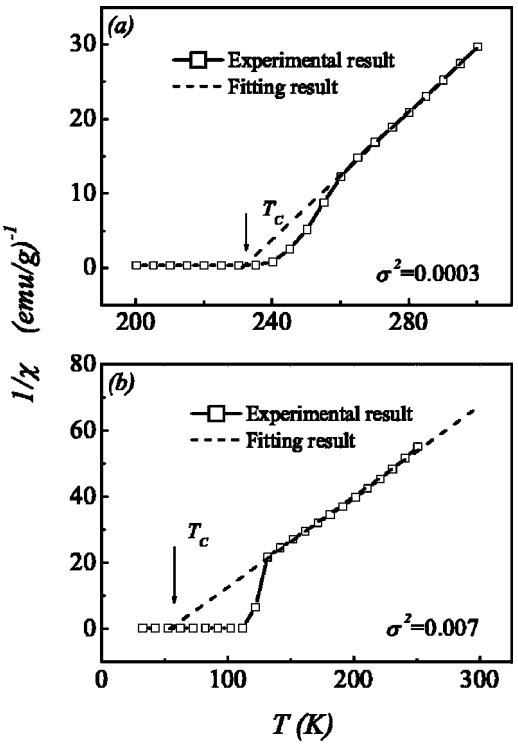

FIG. 10. Inverse susceptibility $1/\chi$ as a function of T for the samples with (a) $\sigma^2=0.0003$ and (b) $\sigma^2=0.007$ measured under $H=100$ Oe. The dashed lines are the fitting results following the Curie-Weiss law. The unit of σ^2 is Å^2.

fitting results using this law. It is clearly shown that the high-T behavior of the two samples is well described by the Curie-Weiss law, and the value of T_C can be determined by extrapolating the high-T data to $1/\chi=0$. We have two types of evidence to identify the existence of the Griffiths phase. First, from the slopes of the two fitting lines, we evaluate the values of S_{eff} to be 8.0 and 4.0, respectively, for the samples of $\sigma^2=0.0003$ and 0.007. These values are much larger than $S_{eff}=1.77$ for an effective Mn ion (the weighted average of $S_{\mathrm{Mn4+}}=3/2$ and $S_{\mathrm{Mn3+}}=2$), indicating that the high-T paramagnetism for the two samples originates from the contributions of individual magnetic entities containing more than two Mn ions, i.e., FM clusters, rather than from the contributions of individual magnetic ions.[39,40] Second, when T is approaching T_C from the high-T side, the $1/\chi$ data deviate from the Curie-Weiss fitting lines, indicating a much larger slope than the fitting line. Therefore, before the system evolves into the cluster-glass state from the FM state with increasing σ^2, there appears a Griffiths phase which is randomly distributed FM clusters at $T>T_C$. Because these FM clusters have larger effective spins than individual magnetic ions, $1/\chi$ as a function of T would show a large deviation from the Curie-Weiss law once the Griffiths phase appears, and can be described by a susceptibility exponent less than unity.[39,41]

In the highly disordered manganites the ground state changes from a metal to an insulator. Our results reveal that the two competition interactions plus the quenched disorder will give rise to a cluster-glass-like behavior or a phase separated state, which may be induced by the enhanced fluctuations between competing interactions. Moreover, such enhanced fluctuation is amenable to an external magnetic field favoring the FMM phase, and then the huge CMR effect is observable at the intermediate disorder case. We thus argue that in the inhomogeneous states, the competition and fluctuations between the ordered ground states at the clean-limit case may be some of the most important ingredients of the CMR and other interesting effects in manganites.

Our results coincide with previous theoretical research and reveal the importance of disorder in manganites. Theoretically, the disorder effects in manganites were extensively studied by Sen and Dagotto.[17,42] They indicated that the effect of quenched disorder on the competition between ordered states separated by a first-order transition will produce a phase diagram with features resembling quantum critical behavior. The low-temperature region consists of coexisting ordered clusters.[42] The disorder can induce the insulator-metal-insulator transition simultaneously.[17] Our experiments illustrated these features, and the A-site disorder induces the transition of the ground state from FMM to cluster-glass insulator, which probably is a quantum phase transition because the transition is the ground state and close to 0 K. Surely, a physically sound explanation on the observed results in the present work still needs more direct evidence for the existence of short-range magnetically ordered region. Our results indicate that the A-site disorder is an important ingredient for understanding the CMR physics and phase separation in manganites.

IV. CONCLUSIONS

In conclusion, a series of manganite compounds, with a constant average A-site ionic radius but different variances of the A-site ionic radii σ^2 from 0.0003 to 0.015, have been investigated using various experimental techniques. Our results have shown that all the samples have the orthorhombic crystallographic structure and no change of lattice parameters is observable from the XRD technique. Therefore, the lattice effects in our system are weak. The increasing A-site disorder characterized by variance of σ^2 results in the following effects: (i) the ferromagnetic transition temperature and magnetization of the samples decrease significantly; (ii) an irreversibility between the ZFC and FC magnetizations against temperature appears and the system transforms from ferromagnetic state to cluster glass-state; (iii) an abrupt MIT of the ground state is confirmed and a good $\ln \rho \sim T^{1/4}$ relationship (VRH) for the high-disordered samples is observed; (iv) the M-H curves of the sample with intermediate disorder ($\sigma^2=0.008$) exhibit a sharp stepwise behavior at a field $H \sim 3.5$ T.

A phase separation scenario is used to explain these experimental effects. With increasing A-site disorder, the random oxygen displacements and then random local radial distortions of the MnO_6 octahedra become significant and the Mn-O-Mn bond angle becomes smaller. The A-site disorder brings about the electron localization that burdens the Mn-O-Mn double-exchange interaction mediated by the conduc-

tion electrons. The long-range FM ground state at $\sigma^2 < 0.007$ loses its dominance to the short-range magnetically ordered state as $\sigma^2 > 0.008$. The disorder and the competing interactions are responsible for the occurrence of spin clusters, and the weak magnetic interaction between these clusters leads to the cluster-glass-like behavior.

ACKNOWLEDGMENTS

This work was cosupported by the Natural Science Foundation of China (50332020, 10021001, 50528203) and National Key Projects for Basic Research of China (2002CB613303, 2004CB619004).

*Author to whom correspondence should be addressed. Email address: liujm@nju.edu.cn

[1] Y. Tokura and N. Nagaosa, Science **288**, 462 (2000).
[2] E. Dagotto, T. Hotta, and A. Moreo, Phys. Rep. **344**, 1 (2001).
[3] S. Jin, T. H. Tiefel, M. McCormack, R. A. Fastnacht, R. Ramesh, and L. H. Chen, Science **264**, 413 (1997).
[4] C. Zener, Phys. Rev. **82**, 403 (1951).
[5] A. J. Millis, P. B. Littlewood, and B. I. Shraiman, Phys. Rev. Lett. **74**, 5144 (1995).
[6] S. Murakami and N. Nagaosa, Phys. Rev. Lett. **90**, 197201 (2003).
[7] M. Uehara, S. Mori, C. H. Chen, and S.-W. Cheong, Nature (London) **399**, 560 (1999).
[8] A. Moreo, S. Yunoki, and E. Dagotto, Science **283**, 2034 (1999).
[9] D. Akahoshi, M. Uchida, Y. Tomioka, T. Arima, Y. Matsui, and Y. Tokura, Phys. Rev. Lett. **90**, 177203 (2004).
[10] S. M. Yusuf, M. Sahana, K. Dörr, U. K. Rößler, and K.-H. Müller, Phys. Rev. B **66**, 064414 (2002).
[11] S. Rößler, U. K. Rößler, K. Nenkov, D. Eckert, S. M. Yusuf, K. Dörr, and K.-H. Müller, Phys. Rev. B **70**, 104417 (2004).
[12] J. M. DeTeresa, P. A. Algarabel, C. Ritter, J. Blasco, M. R. Ibarra, L. Morellon, J. I. Espeso, and J. C. Gómez-Sal, Phys. Rev. Lett. **94**, 207205 (2005).
[13] S. Nair and A. Banerjee, Phys. Rev. Lett. **93**, 117204 (2004).
[14] A. Barnable, Appl. Phys. Lett. **71**, 3907 (1997).
[15] T. Kimura, Y. Tomioka, R. Kumai, Y. Okimoto, and Y. Tokura, Phys. Rev. Lett. **83**, 3940 (1999).
[16] Y. Motome, N. Furukawa, and N. Nagaosa, Phys. Rev. Lett. **91**, 167204 (2003).
[17] C. Sen, G. Alvarez, and E. Dagotto, Phys. Rev. B **70**, 064428 (2004).
[18] J. Burgy, M. Mayr, V. Martin-Mayor, A. Moreo, and E. Dagotto, Phys. Rev. Lett. **87**, 277202 (2001).
[19] L. M. Rodriguez-Martinez and J. P. Attifield, Phys. Rev. B **54**, R15622 (1996).
[20] L. M. Rodriguez-Martinez and J. P. Attifield, Phys. Rev. B **58**, 2426 (1998).
[21] Y. Tomioka and Y. Tokura, Phys. Rev. B **70**, 014432 (2004).
[22] K. F. Wang, Y. Wang, L. F. Wang, S. Dong, H. Yu, Q. C. Li, J.-M. Liu, and Z. F. Ren, Appl. Phys. Lett. (to be published).
[23] R. D. Shannon, Acta Crystallogr., Sect. A: Cryst. Phys., Diffr., Theor. Gen. Crystallogr. **A32**, 751 (1976).
[24] J. Blasco, J. García, J. M. de Teresa, M. R. Ibarra, J. Perez, P. A. Algarabel, C. Marquina, and C. Ritter, Phys. Rev. B **55**, 8905 (1997).
[25] J. W. Cai, C. Wang, B. G. Shen, J. G. Zhan, and W. S. Zhan, Appl. Phys. Lett. **71**, 1727 (1997).
[26] H. Y. Hwang, S.-W. Cheong, P. G. Radaelli, M. Marezio, and B. Batlogg, Phys. Rev. Lett. **75**, 914 (1995).
[27] J. A. Mydosh, *Spin glasses: An Experimental Introduction* (Taylor & Francis, Washington, D.C., 1993).
[28] N. Furukawa, J. Phys. Soc. Jpn. **64**, 2734 (1995).
[29] N. Furukawa, J. Phys. Soc. Jpn. **64**, 2754 (1995).
[30] Guixin Cao, Jincang Zhang, Shixun Cao, Chao Jing, and Xuechu Shen, Phys. Rev. B **71**, 174414 (2005).
[31] D. Zhu, B. Raveau, A. Maignan, M. Hervieu, V. Hardy, and C. Martin, J. Appl. Phys. **95**, 4245 (2004).
[32] A. Maignan, S. Hebert, V. Hardy, C. Martin, M. Hervieu, and B. Raveau, J. Phys.: Condens. Matter **14**, 11809 (2002).
[33] R. Mahendiran, A. Maignan, S. Hebert, C. Martin, M. Hervieu, B. Raveau, J. F. Mitchell, and P. Schiffer, Phys. Rev. Lett. **89**, 286602 (2002).
[34] V. Hardy, S. Majumdar, S. J. Crowe, M. R. Lees, D. McK. Paul, L. Hervé, A. Maignan, S. Hébert, C. Martin, C. Yaicle, M. Hervieu, and B. Raveau, Phys. Rev. B **69**, 020407(R) (2004).
[35] J. R. Sun, J. Gao, Y. Fei, R. W. Li, and B. G. Shen, Phys. Rev. B **67**, 144414 (2003).
[36] L. Ghivelder, R. S. Freitas, M. G. dasVirgens, M. A. Continentino, H. Martinho, L. Granja, M. Quintero, G. Leyva, P. Levy, and E. Parisi, Phys. Rev. B **69**, 214414 (2004).
[37] N. Mott, *Conduction in Non-Crystalline Materials* (Clarendon, Oxford, 1993).
[38] M. Jaime, H. T. Hardner, M. B. Salamon, M. Rubinstein, P. Dorsey, and D. Emin, Phys. Rev. Lett. **78**, 951 (1997).
[39] A. H. Castro Neto, G. Castilla, and B. A. Jones, Phys. Rev. Lett. **81**, 3531 (1998).
[40] M. B. Salamon, P. Lin, and S. H. Chun, Phys. Rev. Lett. **88**, 197203 (2002).
[41] A. J. Bray, Phys. Rev. Lett. **59**, 586 (1987).
[42] J. Burgy, M. Mayr, V. Martin-Mayor, A. Moreo, and E. Dagotto, Phys. Rev. Lett. **87**, 277202 (2001).